SEISMIC BEHAVIOR OF LIGHTLY REINFORCED CONCRETE BEAM-COLUMN JOINTS AT FIRST FLOOR

Panuwat Joyklad [1] and Amorn Pimanmas [2]

[1] Lecturer, Department of Civil Engineering, Kasem Bundit University, joy.civil@gmail.com

[2] Associate Professor, Sirindhorn International Institute of Technology, Thammasat University, amorn@siit.tu.ac.th

ABSTRACT

An extensive experimental test has been conducted in the order to investigate the performance of interior reinforced concrete beam-column connections subjected to lateral earthquake loading. In the past, however, most experimental programs were paid attention to individual beam-column connection specimens particularly in cruciform configuration. Those typical tested programs have been made on the assumption that the inflection points were located at middle length of columns and beams. In real behavior of structure, especially in the first floor building, the inflection point may not stay at mid of column height because the relative stiffness between beam-column connection and fixed foundation is difference. Disparity of actual behavior and classical assumption affect the behavior for both beam-column connection and column. This paper presents an experimental study of intermediate lightly RC frame subassemblies. Four specimens were cast and divided into two series. These two series have the same dimension and reinforcing details except that the columns in second series were extended twice times from the beam-column connection and fixed to foundation base. The specimens in second series intended to represent the 1st floor of interior building frames. The different behavior of specimens in these series was described experimentally. Based on observed behavior, it can be understood that the inflection point in column at bottom story of building frame plays the important role for behavior of both beam-column and column. In addition, the study results can also be used as informative data for further researches.

KEYWORDS: beam-column joint, column, inflection point and shear failure

1. INTRODUCTION

More than half a century, numerous of experimental researches focused on behavior of reinforced concrete subassemblies under reversed cyclic loading have been carried out. Column and beam-column connection have been both selected as critical elements of structure because high stress concentrations are induced during seismic excitation while the entire gravity loads of building are also thoroughly transmitted to these elements. In the past, however, the behavioral studies of beam-column connections and columns have been performed separately. In the case of beam-column connection, although the forms of specimens have been captured differently based on research demands for example wide-beam to column [1], double beam-column connection interact with beam span [2] and beam to wide-column [3], but in general configuration of tested specimens for representing a interior beam-column connection is cruciform (Figure 1 (a)). The length of beams and columns were specified equal to distance of inflection point which generally assumed to locate at the mid length of beams and columns of the real structure. The testing in such style is easily to perform and, moreover, these subassemblies are determinate, the force acting on the joint can be rapidly computed [4, 5, 6]. As a result, the current understanding of the behaviour and the procedures for the design of beam-column connections are most entirely based on observation and conclusions drawn from such tests on individual beam-column connection.

In the case of column, the single curvature and double specimens have been mostly used [7] to evaluate the seismic performance of column. The key influences for selecting a type of specimen depend on a capable of laboratory and need of research accuracy (Figure 1 (b) and (c)). It should be pointed out that the single curvature specimens, cantilever type, are somewhat popular than double curvature because it is convenient to construct and control during testing times.

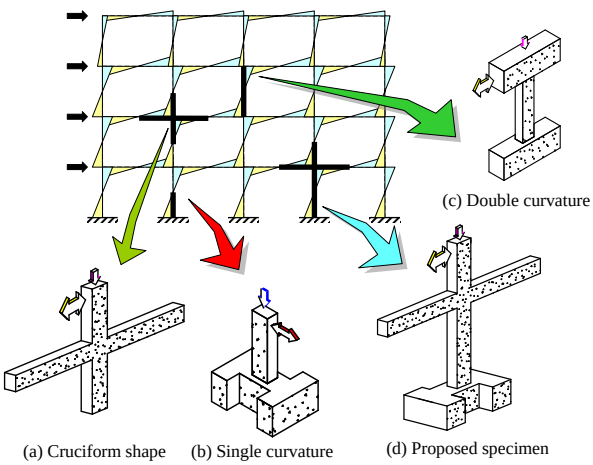

Figure 1 Typical RC subassembly specimens

However, it can be found that the responses of beam-column connection and column in the real RC structure under laterally loaded by earthquake, especially in the first few floors, do not comply with previous assumptions. Based on elastic behaviour, the contraflexure point can be located anywhere between mid to full height of column depends on relative stiffness between beam-column connection and column. Figure 2 shows the schematic bending moment diagram of three hypothesis buildings under lateral load. The depth of columns is varied from 0.5, 1.0, and 2.0 times compared to depth of beams, respectively. It is noteworthy that the inflection point is located close to mid of column high for building with small column dimension (Figure 2 (a)) while it is moved upwards to the are increased (Figure 2 (b) and (c)).

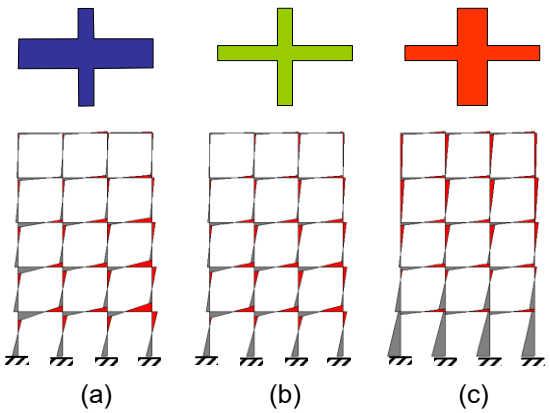

Figure 2 The variation of inflection point (a) small columns and large beams, (b) medium beams and columns, and (c) large columns and small beams

As illustrated in the previous example, responses of beam-column connection and column in real structure may not agree with assumed for conventional laboratory tests. Therefore, the individual study on beam-column connection or column may be misunderstanding on actual behavior of those components. Due to the lack of relevant studies, the intensive research focused on beam-column joint included column shall be performed for make clear understanding in interaction behavior between these two members.

The significant of this research is combining a lightly reinforced concrete column and beam-column connection (Figure 1 (d)). Therefore, the interaction behavior based on relative stiffness between these two elements can be investigated experimentally. Since the past international researches focused on combined behaviors of column and beam-column connection are still limited. Even through, some experimental reports studied on behaviors of confined beam-column connections interact with columns are allowable but the deep discussion and explanation were not clearly presented [8, 9]. Hence, the experimental results of this research can be used for additional data base of subassembly tested specimens.

This paper presents the results of an experimental investigation in which the behavior of beam-column connections and column are studied under earthquake-type loading both by conventional cruciform beam-column connections, as has been done in the previous researches, and by proposed frame subassemblies which represented a first story of RC building frame. The reinforcing details and structural geometry of tested specimens, moreover, were constructed based on collective data from surveying of structural drawing of existing buildings in Bangkok [10]. The study focused on reinforced concrete frames having 5-21 stories. The building occupancy type included university, school, apartment, governmental office and hospital. The prototype buildings were designed for gravity loads only based on the non-seismic provisions of the ACI318 code. The outstanding of this research which specimens were constructed from existing structures is that the behavior of these specimens can exactly represent close to behavior of real structure. The main characteristics of the specimens were that no transverse reinforcements were provided in joint core while lightly amount of ties was reinforced in the column. There are generally termed as lightly (LRC) structures. In the experiment, the specimens were grouped according to tributary area concept. There are two tributary area types used in this paper. The medium tributary represents for medium rise buildings while the small tributary area stands for low rise buildings, respectively. Hence, size of columns which received higher axial load was

larger than the column which received lower axial load while the size of beams was still kept the same.

2. TEST PROGRAM

2.1 SPECIMEN DETAILS

Figure 3 shows the details of the four ½-scale LRC test specimens. They label as JM, JS, CJM, and CJS. JM and JS stand for cruciform beam-column joints and these two specimens are grouped in the first series. The specimens represent to medium and small tributary area, respectively (Figure 3 (b)). The column cross-section dimension for JM of 200x350 mm, and the beam cross-section dimension of 175 x 300 mm. The column cross-section for JS of 200 x 300 mm, the beam cross-section dimension is identical as JM. It should be pointed out that the depth of column section for JS has smaller size compared to JM due to column tributary area concept. Next, the specimen in second series, CJM and CJS stand for frame subassemblies. They were designed identically with JM and JS, respectively. The disparity is that the column is extended twice time from the beam-column connection. The specimen in second series is assigned to represent the interior frame in the bottom story of prototype buildings.

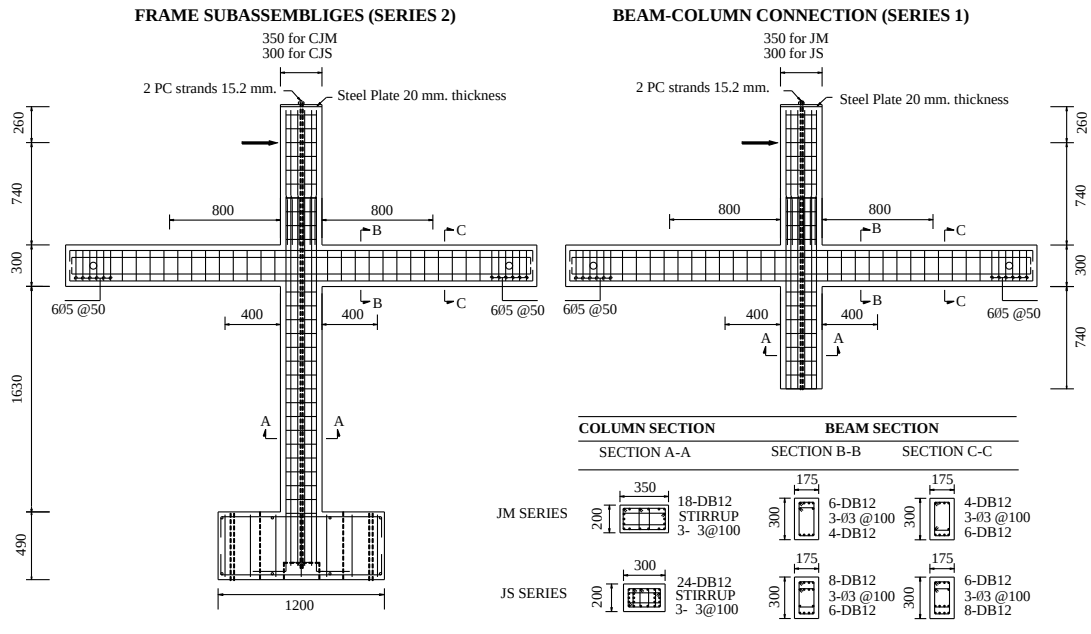

Figure 3 Dimension and reinforcing details of tested specimens

2.2 MATERIAL PROPERTIES

Longitudinal reinforcement for the beams and columns consisted of 12 mm of diameter of deformed bars and were characterized by yield strength f_y of 495 MPa. The transverse reinforcement of all specimens comprised of 3 mm of diameter of mild steel bars and was characterized by yield strength f_y of 518 MPa. The average compressive strength of concrete, f_c', observed from the concrete cylinder samples, was found to be 28.16 MPa and 26.18 for columns and beams of JM and CJM, respectively, while 24.51 MPa and 25.07 MPa were also found for columns and beams for JS and CJS, respectively.

2.3 TEST SETUP

The test set-up and boundary conditions are shown in Figure 4. The lateral forced displacement was applied at the top of the column through a 500 kN hydraulic actuator. The ends of beam were supported by rollers that allowed free horizontal movement to simulate lateral drift. The axial load for representing sustained gravity force was applied to the column by means of vertical prestressing. The amounts of vertical force in columns are obtained from the average value of surveying data [10] and are shown in Table 1. The column was pushed forward and pulled backward in a reversed cyclic pattern with the target lateral drifts of 0.25%, 0.50%, 0.75%… as shown in Figure 5. The target loop was repeated twice for each drift level. The load was continued until and beyond the peak load to trace the post-peak behavior. The tests were stopped when the load carrying capacity drop less than 80% of maximum load [11]. The strains of reinforcements during the test were measured by strain gauges attached at the reinforcement surfaces. Beams and column rotation, shear deformation of the joint were measured by LVDTs located at specified location as shown in Figure 6.

2.4 STRUCTURAL INDICES

Table 1 summarizes the structural indices of the specimens. They were estimated using the tested material properties and in accordance with the recommendation provided by ACI [12]. In the case of lightly reinforced concrete column, for taking into account on strength decay due to reversed cyclic loading, shear capacity of tested specimens was evaluated by proposed equation of Sezen and Moehle [13]. The joint shear forces were calculated based on the yielding of beam reinforcements. Joint shear strengths for existing structure, without

transverse reinforcement in the connection, were computed by formula recommended of ATC40 [14]. In order to investigate bond characteristics, the bond index was also prepared. The value of beam bar bond index recommended by Kitayama et. al. [15] is 4.50 or less for good bond anchorage. An index J, joint failure index, is a indication of concrete strength relative to the joint shear stress at beam yielding. It is expected that J greater than 1.0 would result in premature joint shear failure, while J less than 1.0 would probably lead to beam yielding [16]. It should be notified that the shear span, a, is the most important parameter for evaluating the behavior of RC frame subassemblies. In specimen JM and JS, it was assumed to equal of clear depth of bottom column. Since, these specimens were firstly assumed that the inflection point in the column is shared equally. While, the shear span for specimens in second series was measured from the fixed base of column to the point of inflection. The formula uses for primary predicting of shear span of subassemblies can be analyzed based on conventional elastic approach. For sake the simplicity, however, the homogeneous of material were established at the beginning, in addition the length of left and right were also assumed to be equal and denoted as L. Hence,

$$a = \frac{(h_t + h_b)LI_c + 3h_b^2 I_b}{LI_c + 6h_b I_b} \quad (1)$$

Where h_t and h_b is the length of top and bottom column measured from the connection center, respectively. The moment of inertia of beams and columns were defined as I_b and I_c, respectively.

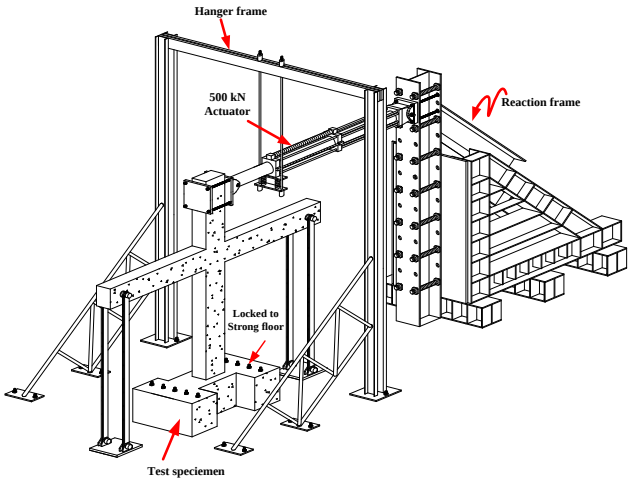

Figure 4 Schematic test set-up of specimen in second series

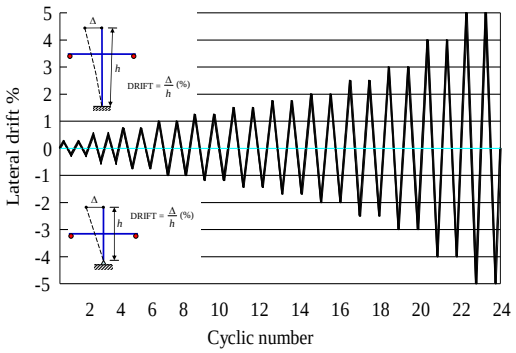

Figure 5 Displacement history of specimens

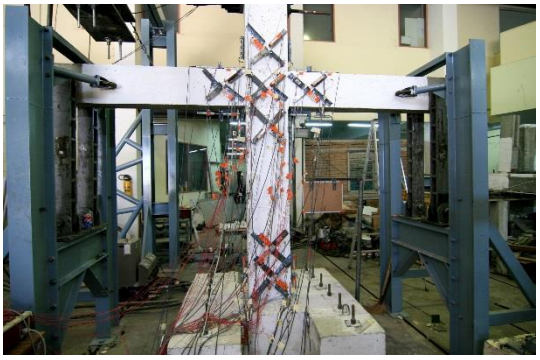

Figure 6 Photo of test set-up

Table 1 Design parameters

Code / Indices	JM	JS	CJM	CJS
a (m)	0.74	0.74	1.23	1.11
$P/A_g f'_c$	0.18	0.20	0.17	0.19
$\sum M_{nc}/\sum M_{nb}$	2.20	1.67	2.33	1.67
V_{ju}/V_{jn}	1.52	2.59	1.51	2.73
M_{nb}/aV_{nb}	0.61	0.74	0.47	0.58
M_{nc}/aV_{nc}	1.40	1.53	0.98	1.16
BI	2.80	2.82	2.91	3.02
J	0.56	0.81	0.64	1.00

Based on structural indices postulated in Table 1, the primary mode of failure can be predicted. The axial force ratios for all specimens show very low values therefore the high potential failure from axial compressive load is automatically moved. Even through, the column compressive force is significantly affected to joint shear cracking but the variation of compressive loads of specimens are too small therefore the effect form axial compressive load on test specimen can be neglected. The column-to-beam flexural ratios were greater than 1.4 for all specimens. Based on conventional capacity design concept and recommendation by NZS3101 [17], the column hinging is theoretically proscribed. Even through the shear failure in the column may significant since the normalized flexural-to-shear strength ratios of columns were greater than one. However, the presence of high column-to-beam flexural strength ratios show high elastic behavior column and, therefore, column shear failure may less probable to occur. In contrast, the shear failure in beams is already prevented by low value of normalized flexural-to-shear strength ratios. In a view of bond behavior, according to **BI** less than 4.5, there is satisfying the good bond condition. In addition, all specimens show the high probably of join shear failure because the ratio of joint shear forces and joint shear capacities is higher than 1.0. However, the joint failure index indicated that the probability of joint shear failure before beam bars yielding may appear for JS and CJS while the JM and CJM attained the joint shear failure after yielding of beam bars. The objective for describing on structural indices of both series, since it really to check

that simple evaluation method for simple beam-column connection can be applied to frame subassemblies or not. The discussion of this issue will be explained in more detail in the last section.

3. DESCRIPTION OF TEST BEHAVIOR

The general behaviors of the test specimens were identified based on the load-displacement hysteresis response, the visible crack patterns, and the local strain recorded from the reinforcements. Figure 7 shows the horizontal story shear force versus horizontal displacement hysteresis loops of all specimens. The crack patterns observed during the test are shown in Figure 8. Figure 9 illustrates the local damages at column of CJM and CJS specimens. The strain distribution on bottom longitudinal bars of beams and main longitudinal bars of column are presented in Figure 10 and Figure 11, respectively. The normalized joint shear stress is presented in Figure 12. Finally, the bond anchorage force versus drift ratio is exhibited in Figure 13.

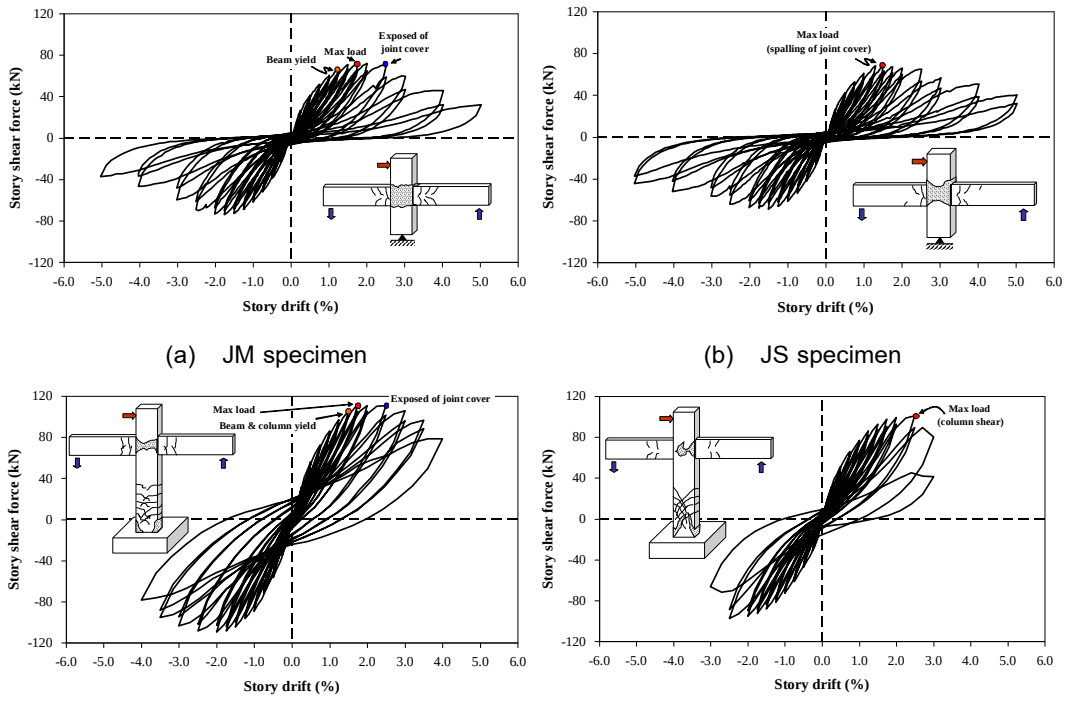

(a) JM specimen (b) JS specimen

(c) CJM specimen (d) CJS specimen

Figure 7 Hysteresis loops

3.1 Specimen JM

First flexural cracks were detected in the beams at 0.25% drift. The cracks from top and bottom fiber of beam sections were jointed together as subsequent loading. At the 0.50% drift, the cracks were extended the length and width, moreover, the diagonal tensile cracks were firstly found in the joint. Consequently, the initial yielding of beam reinforcements was firstly recorded at 1.00% drift (Figure 10 (a)). The maximum load was 71.79 kN, attained in the drift ratio of 1.75% (Figure 7). Although the column shear force reached the maximum point but the stresses in beam bars still maintained the load, the gradual reduction of column shear force was found in hysteresis loop during 1.75% to 2.50% drift ratio. After 2.50% drift ratio, no new cracks occurred in beams. The diagonal cracks in the joint core continued to widen and spalling of concrete cover was seriously presented. The exposed of column longitudinal bars in the joint core and spalling of concrete at the joint corner were observed of a drift at 3.00%. It can be seen that, beyond 3.0% drift ratio, the column shear force started to drop rapidly. The parallel behavior can be observed for joint shear force as plotted in Figure 12 (a). The calculated anchorage of JM is illustrated in Figure 13 (a). It can be observed directly that the anchorage force increased as subsequent cyclic loading. The maximum anchorage force attained before maximum column shear force and slowly decay since 1.25% drift ratio (Figure 13 (a)). Even thought the yielding was observed to penetrate in the joint core (Figure 10 (a)) but the anchorage force can be maintained, and bond deterioration did not appear throughout the test. As a result, it can be suggested that the failure of specimen is joint shear failure after yielding of beam reinforcements. Due to the brittle failure by joint shear, the specimen behaved a significant pinching hysteretic loop throughout the test.

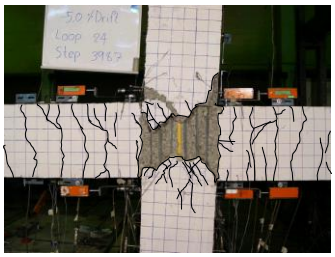

(a) JM

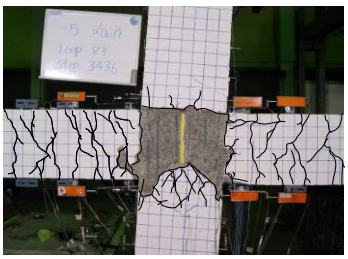

(b) JS

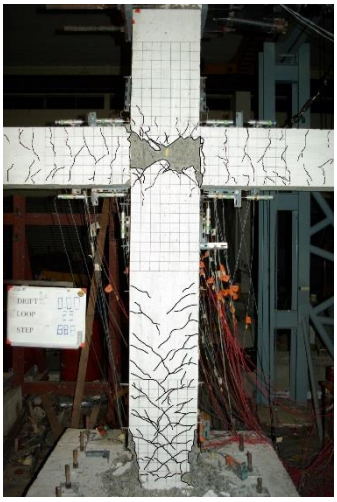

(c) CJM

(d) CJS

Figure 8 Crack patterns

(a) CJM

(b) CJS

Figure 9 Local damage in column of CJM and CJS

3.2 Specimen JS

Specimen JS was an interior beam-column connection with smaller column depth compared to JM. The flexural cracks initiated in beams during 0.25% drift. These vertical cracks extended and jointed together at the middle zone of beams as subsequent drift ratio.

At 0.50% drift, the first diagonal tension cracks were observed in the joint core. When the drift ratio was increased to 0.50% and 1.50%, respectively, the diagonal cracks in joint zone increased rapidly and no significant flexural cracks were detected in the beams. Joint shear cracks were opened widely followed by spalling of concrete cover at the end of 1.50% drift. The maximum load of 68.10 kN, which was attained at the first cycle of drift ratio of 1.50%. The maximum column shear force decreased gradually. After maximum strain of beam bars were reached at 2.50% drift, the column shear force started progressive deteriorating as illustrated in Figure 7 (b). Hence, the mode of failure of JS can be classified as joint shear failure before yielding of beam reinforcement (Figure 10 (b)). The anchorage force in the joint was developed with the same trend of column shear force. That is, the anchorage force in the joint was decreased rapidly after column shear force attained the maximum force at 1.50% drift. This may be explained by the changing of compressive strain to tensile strain as increased drift ratio. The compressive strain was gradually changed to tensile which may be contributed from imperfect closing of pull-out crack at the beam section close to column faces. As a result, the compressive stress in the compression reinforcement was reduced slowly and lead to decaying of bond force as shown in Figure 13 (b). It can be noted that the joint shear stress and anchorage force were developed independently. The specimen also displayed the pinching behavior similar to JM specimen.

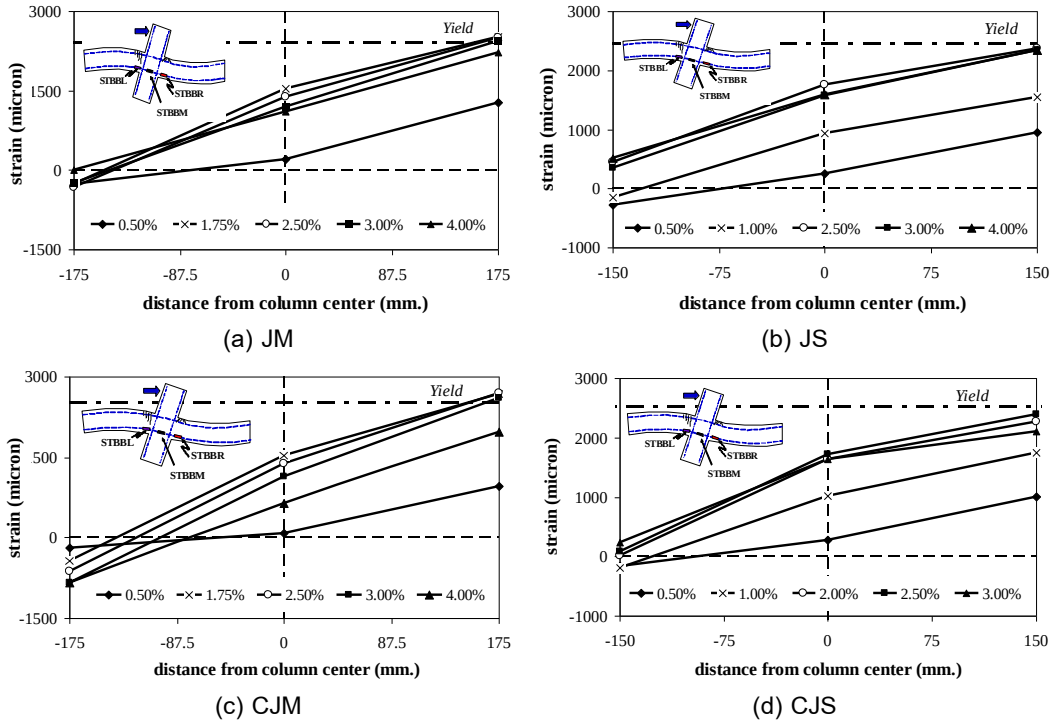

(a) JM (b) JS

(c) CJM (d) CJS

Figure 10 Local strain in beam bottom bars

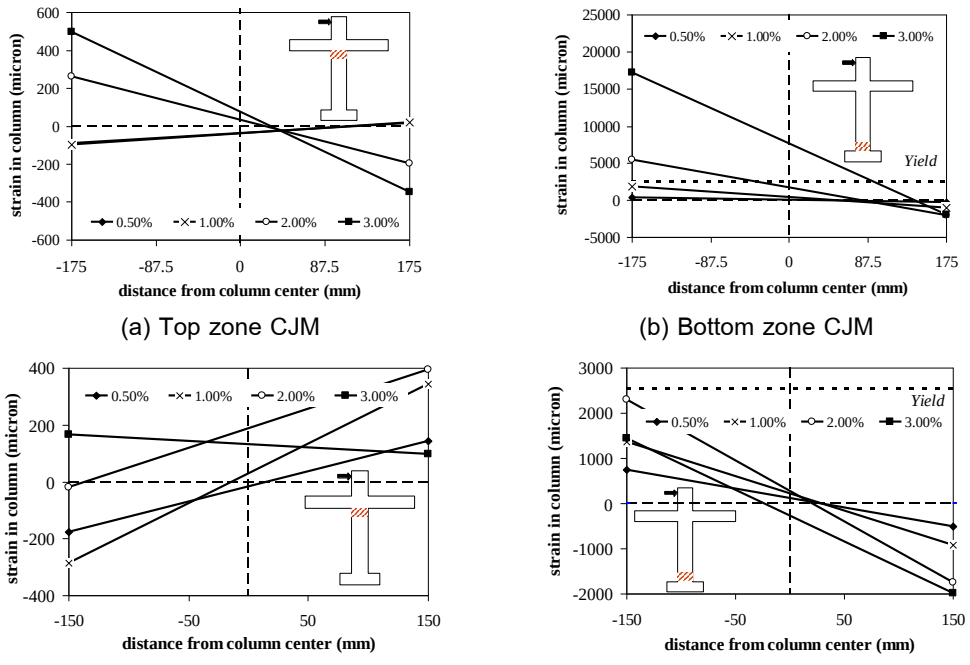

(a) Top zone CJM (b) Bottom zone CJM

(c) Top zone CJS (d) Bottom zone CJS

Figure 11 Local strain in column bars of CJM and CJS

3.3 Specimen CJM

The crack patterns of specimen CJM is shown in Figure 8 (c). The flexural cracks in beams and columns observed at beginning of 0.50% drift and slight vertical cracks at mid of joint core can be detected at the end this drift. When a drift of 0.75% was attained, diagonal cracks in joint zone were displayed clearly. They formed an X-pattern at the end of this drift ratio. As the drift ratio increased, more cracks were found to propagate rapidly at the beams. At drift ratio of 1.50%, the tensile strains of beams and column at base, were reached the yielding point (Figure 10 (c) and 11 (b)). Until drift ratio of 1.75%, the specimen reached its maximum capacity of 112.38 kN (Figure 7 (c)). At the same drift level, the spalling of concrete cover at the joint can be detected. As observed from Figure 7 (c), during 1.75% to 2.50% drift ratio, the column shear force degraded slowly as a result of steady strain development. The crack in column base continued to grow until the drift ratio beyond 2.50%, the concrete at bottom base of column started to crush. After this drift level, the measured strain in beam reinforcing bars drastically dropped (Figure 10 (c)), this can be investigated together with rapidly reduced of column shear force (Figure 7 (c)). In the subsequent inelastic cycle, the damage was concentrated at the compression zones of column base, until the drift ratio attained 3.50%, the splitting cracks along longitudinal bars of column were formed. The testing program was stopped at the drift ratio of 4.00% because the concrete cover of column at the compression zones were met the serious damage and followed by buckled of main column reinforcement (Figure 9 (a)). The failure of specimen CJM governed by joint shear failure and followed by flexural failure of column section at base (Figure 8 (c)). It should be notified that the hysteresis loop behavior of specimen CJM is larger compared to JM. The joint shear force was normalized and shown in Figure 12 (a). It can be seen that joint shear force increased gradually even thorough column shear force decreased. This may result from strain in beam can be maintained stationary while the column shear force slowly dropped (Figure 12 (a)). However, the anchorage force started to degrade after specimen attained the maximum column shear force (Figure 13 (a)).

3.4 Specimen CJS

The behavior of CJS specimen from 0.25% - 0.75% drift ratio was similar to CJM except that the flexural cracks in bottom column were extended and inclined to form the flexural -

shear cracks at the end of 0.75% drift ratio. The flexural cracks in beams were rarely to observe while distributed alternate diagonal cracks in the beam-column joint were formed aggressively. It is noteworthy that the spread diagonal cracks in the connection were formed X-shape at the end of this drift level. At the beginning of 1.00% drift ratio, the inclined flexural cracks from tension side of bottom column extend diagonally to compression side.

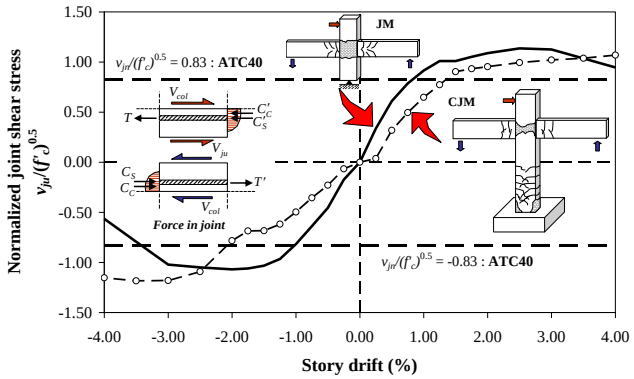

(a) Specimens JM and CJM

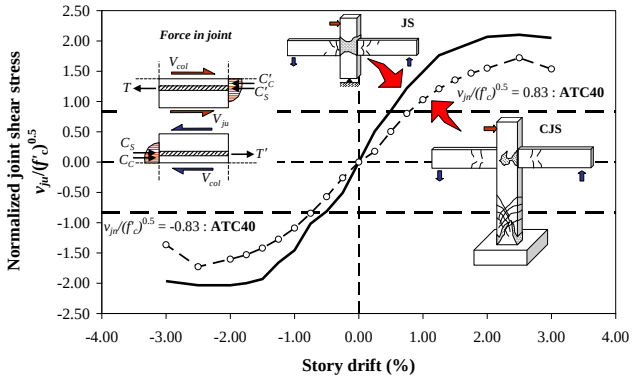

(b) Specimens JS and CJS

Figure 12 Normalized joint shear stresses

During 1.25% - 2.00% of drift ratio, small pieces of concrete cover the joint started to fall down while the inclined cracks of bottom column continued to grow. However, as drift ratio increased, no more cracks were found to propagate in beams. The concrete joint cover was exposed largely at the beginning of 2.50% drift ratio. The maximum column shear force was 100.79 kN at a drift ratio of 2.50% (Figure 7 (d)). At 3.00% drift, the large diagonal shear

crack formed in the bottom column, concrete cover at the sides of column spalled and the column volumetric expended rapidly (Figure 8 (d) and Figure 9 (b)). The testing program was stopped according to instability of column lead from serious shear failure were took place. In addition, until the end of the experiment, the yielding of reinforcements in longitudinal column and beams were not observed (Figure 10(d)). As a result of two brittle failure mechanisms occupied the performance of specimen CJS therefore the pinching behavior of hysteresis loop and suddenly collapse of strength was presented (Figure 7 (d)). The behavior of joint shear force was similar to column shear force as depicted in Figure 12 (b). The joint shear force increased as drift ratio increased until the maximum column shear force was attained, the joint shear force also started to decay. The bond anchorage strength had similar trend as column shear force and joint shear force. It reached the maximum strength at 2.50% drift ratio and dropped gradually (Figure 13 (b)).

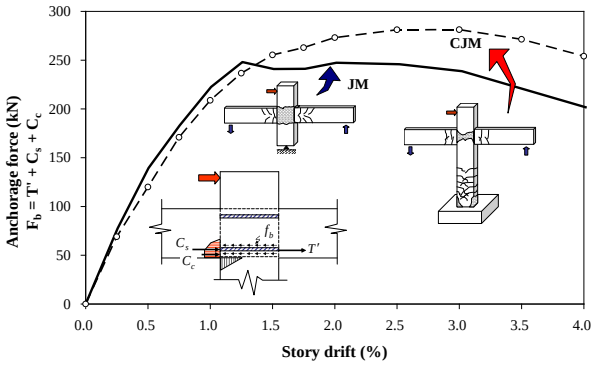

(a) Specimen JM and CJM

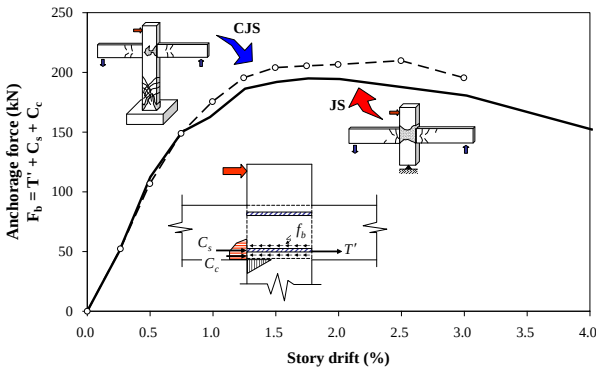

(b) specimen JS and CJS

Figure 13 Anchorage force in the joints

4. DISCUSSION OF TEST RESULTS

As depicted in Figure 7 (a) and (c), the column shear force between specimen in 1st and 2nd series were significantly difference. The maximum disparity is 77.81% and 55.37% for M series and S series, respectively. These emphasize on the major effect contributed from column which was fixed at base to beam-column connection. Since the column shear force can be estimated by equilibrium of forces around joint as illustrated in Figure 14 (a). The calculated column shear force is identified elastically by following relation,

$$P_{cal} = R\left(\frac{2L}{h_t + h_b}\right) \tag{2}$$

The reaction R is computed by dividing the minimum moment capacity of beam section adjacent column face, normally designed by positive moment, with beam moment arm. In the case of conventional assumption, the length of h_t and h_b are set to equal therefore the column shear force depends on magnitude of developed moment in beam section adjacent the column faces. However, especially in the lowest floor of building, h_t and h_b is not necessary equal due to the different of relative stiffness between beam-column connection and fixed column. The h_b normally is less than half of column height because the larger shear span present in the lower column. Therefore, follow by equation (2), the column shear force can be increased in the case of lower frame subassemblies.

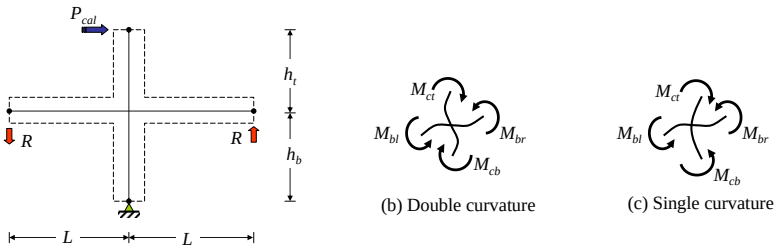

(a) Reaction in beam-column joint

(b) Double curvature

(c) Single curvature

Figure 14 equilibrium of a joint

For specimen CJM and CJS, the location of inflection point can be estimated by similar triangle of bending moment diagram in the lower column. Due to the developed moments

relate directly to strains which recorded from the reinforcing bars (Figure 11) and by moment curvature relationship, hence, the inflection point can be computed experimentally. The variation of inflection points are plotted in Figure 15. The curve shows the movement of inflection point base on shear span of lower column versus drift ratio. The dot lines present predicted column shear span follows by equation (1). In the case of simple cruciform specimens, JM and JS, the ratio of a/h_2 are set equal to 0.5 because of equal of column bending moments is assumed. It can be seen from the Figure 15 that the location of inflection points are located stationary only in the first few drift ratio after that it can move upward to joint zone. In this case, a/h_2 ratio equal to 1.0. According to column section of CJM specimen is larger than CJS while the beam sections are identical, therefore the higher relative stiffness of column compared to beam-column connection are presented for CJM. As a result, the higher shear span in lower column is found for CJM rather than CJS. Thus, h_b for CJM is shorter than CJS and developed higher column shear force as explained previously. It can be investigated by Figure 11 (a) and (b) that the double curvature in lower column for CJM were terminated after 1.50% drift ratio at the same time of strain measured from the top section of column switched the sign convention to be the same as base section. In was noticeable that the drastic movement of inflection started after longitudinal reinforcement in beam reached the yield point at 1.50% drift ratio (Figure 10 (c)).

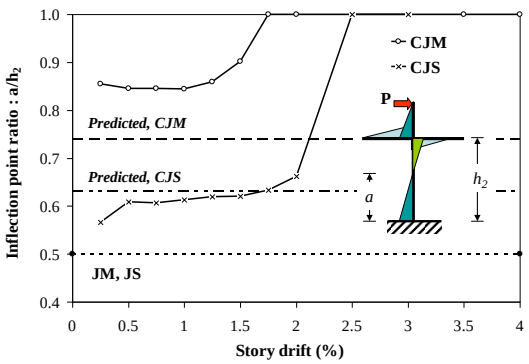

Figure 15 Variation of inflection points

In addition for CJM, the significant relocation of inflection were took place again after joint shear cracks appeared evidently in the joint zone at 1.75% drift ratio. The damage of joint core and yielding of beam sections reduced the beam-column connection stiffness and,

consequently, moved up the inflection point into the joint zone. After shear span in the lower column was increased, as a result, the moment demand in the column section at base gained up rapidly. As the double curvature behavior in lower column was transferred to single curvature, the equilibrium the joint was also restarted (Figure 14 (b) and (c)). As aforesaid, even through the yielding of longitudinal reinforcements were attained in 1.50% drift ratio and inflection point continuously moved up to joint zone ($h_b = 0$) but strain in beams which corresponding to developed moment in beams section still maintained therefore the column shear force during 1.50% to 2.50% was quite stable (Figure 7 (c) and 10 (c)). However, beyond 2.50% drift ratio, the measured strain in beams dropped rapidly as a result of decreasing of developed moment in beam sections hence the column shear force was dropped, respectively.

In the case of CJS, the slenderness of column produced low relative stiffness of column compared to beam-column connection therefore the inflection point was deposited close to the mid high of lower column. As a result, shear force in column was increased because high moment gradient were developed. In addition, the high reinforcing ratio in the column section also induced brittle shear failure. In the term of bending moment in lower column, the slenderness of column induced excellently the double curvature of column as illustrated in Figure 11 (c) and (d). The difference of sign convention of measured strain at top and bottom column was shown obviously. The inflection point started to move upward since the initial diagonal shear cracking were found in the joint core at drift ratio of 0.75% (Figure 15). However, the movement was shown gradually corresponding to development of propagated cracks in the joint zone. Since catastrophic of joint shear which induced the great deterioration of beam-column joint portion, the inflection point was gained up automatically to beam-column connection as presented in Figure 15. After the shear span was increased by flying of inflection point, pre-flexural shear cracks in the lower column were extended and column collapses finally by shear failure. The previous explanations show the significant effects contributed from the movement of inflection point to global behavior of frame subassemblages.

In the view of joint shear stress in beam-column joint. The inflection point has been presented the great participation of joint shear failure. Since the joint shear force can be expression by following equation

$$V_{ju} = T + T' - V_{col} \quad (3)$$

where $T + T'$ is the total tensile forces developed at beam sections close to column faces and column shear force (V_{col}) can be obtained directly form the experiment as shown in Figure 12. The Ramberg-Osgood relationship was used to evaluate the stress of beam longitudinal bars from the strains monitored by strain gauges. As aforementioned, the tensile steels at beam section can develop the yield strength for both JM and CJM (Figure 10 (a) and (c)). Although, yield strength of S-series did not attained but approximate near yield strength can be considered as shown in Figure 10 (b) and (d). Therefore, distinct disparity for both specimens in each series based on equation (3) is only column shear force. It is obvious that the higher column shear force presented in CJM and CJS. It can be said that joint shear force in CJM and CJS developed lower than those found in cruciform specimens. This statement supports by less damage of frame subassemblies specimens at beam-column connection compared to simple cruciform specimens (Figure 8). The joint shear forces were normalized by square-root of compressive strength ($\sqrt{f_c'}$) and plotted together with drift ratio (Figure 12). The maximum difference of normalized joint shear stress for positive direction is 88.89% and 45.45% for CJM and CJS, respectively. In addition, the movement of inflection point found in subassemblies specimen was not only reduces joint shear stress but delay joint shear cracking as well. It can be understood easily if the joint shear strength ratio were assigned. As previous described in 2.4, the joint shear strength ratio proposed by ATC40 [14] for planer interior beam-column joint with low confinement was used for example,

$$\frac{v_{ju}}{\sqrt{f_c'}} = 0.83 \quad (4)$$

It can be found that the specimen JM and JS reached the joint shear capacity at 0.94% and 0.53% drift ratio while CJM and CJS attained at 1.48% and 0.85%, respectively (Figure 12). As illustrated in the figure, CJM and CJS specimens attained the joint criteria after JM and JS. The maximum delaying of assumed joint shear strength of CJM & JM and CJS & JS are 57.45% and 60.38%, respectively. The delaying of joint shear cracking may result to stronger hysteresis loop and give more structural energy dissipation.

Based on measured strains from longitudinal beam bars (Figure 10), the relation of anchorage force of beam reinforcements and story drift ratio can be derived. The anchorage force can be defined as the difference of total force in steel bars of two opposite faces of column. This force shows the bond between steel bars and surrounding concrete.

$$F_b = T' + C_s + C_c \tag{4}$$

The envelope of anchorage force of all specimens was compared in figure 13. Specimens JM & CJM and JS & CJS the anchorage force showed similar relation corresponding to strain distribution which recorded strains of longitudinal reinforcements in beams across the column faces. In specimen JM and JS, the anchorage force reached it maximum value around story drift ratio of 1.25% and 1.75%. It was noteworthy that the anchorage force of JM reached the maximum point before maximum column shear force while the maximum anchorage force of JS attained at the same time of maximum column shear force. The deterioration of anchorage force after reached the maximum force for JM and JS contributed from the degrading of the compressive stress in steels since the accumulated tensile strain from previous loads was took place (Figure 10 (a) and (b)). In the case of CJM, the anchorage force can be developed gradually after the maximum column shear force was attained. A little bit higher and longer of anchorage of CJM compared to JM can be described by the existing of compressive strain in compression steels as shown in Figure 10 (a) and (c). The less accumulated tensile strain in compression steel of CJM present the higher compression force in steel and gained the anchorage force compared to JM. The similar explanation can be drawn developed anchorage force of specimens CJS.

The approximate design described in 2.4 is roughly method to forecast mode of failure of structural members. In the case of frame subassemblies, those procedures can achieve if and only if the corrected shear span is determined. Mode of failure of column is strongly influence by column shear span and this also affect to joint shear stress in beam-column connection. However, after relative stiffness was changed, by yielding of flexural members or cracking in concrete, the inflection is also relocated. If the suffering damage takes place at the joint region before at column base, the inflection point will lift up and column section at the base may be subjected to unexpected large bending force than designed. In contrast, if inflection point is dropped by yielding of column section at base, column shear force may

be reduced, and result to low structural energy dissipation. In this case, the nonlinear analysis may require for detecting the exact failure patterns of structure.

5. CONCLUSION

The present investigation is paid attention to behavior of lightly reinforced concrete subassemblies specimens represented the lowest story in building frame compared to convention test specimens. Specimens were constructed based on actual detailing of existing building in low seismicity. Therefore, the behavior obtained from the experimental can be applied directly to real structures. The research has shown that behaviors of simple beam-column connection and beam-column connection with extended column are difference. The column shear force of specimens with column exhibit drastically higher values than convention cruciform specimens. The difference of maximum column shear force of those specimens is 77.81% and 55.37% for medium and small tributary area specimen, respectively. The normalized joint shear stresses of subassemblies specimens showed the lower value than conventional one. The maximum difference of normalized joint shear stress for positive direction is 88.89% and 45.45% for CJM and CJS, respectively. Moreover, the higher performance of anchorage force was also found in specimens with column.

It can be concluded that beam-column joint in lower floor of building frame behaves differently from general beam-column connection in the upper floor of building. The influence of non-stationary of inflection point which related to stiffness of beam-column connection and column plays important role to structural performance. After relocated of inflection point, the unexpected mode of failure may be presented since shear span distance was changed. The approximate design can be performed after elastic inflection point is determined however the post-elastic behavior is also needed to take into account of interaction behavior of beam-column connection and column.

6. ACKNOWLEDGMENTS

The authors are very grateful to The Royal Golden Jubilee Ph.D Programme (PHD/0050/2550) for providing the research fund to carry out the research.

REFERENCES

[1] Hatamoto, H. (1991). **Reinforced Concrete wide - beam - to - column subassemblages subjected to lateral load.** Kajima Technical Research Institute. Tokyo.

[2] Burnett, E. F. P. & Trenberth, R. J. (1972). "Column load influence on reinforced concrete beam - column connection," **ACI Journal. Proceedings.** Vol.69**. (**No.2): 101-109.

[3] Bing, L., Pan, T. C. & Tran C. T. N. (2009). "Seismic behavior of nonseismically detailed interior beam - wide column and beam - wall connections," **ACI Structural Journal.** Vol.106 (No.5): 591-599.

[4] Hanson, N. W. & Conner, H. W. (1967). "Seismic resistance of reinforced concrete beam - column joints," **Journal of the structural Division.** Vol.93 (No.5): 553-560.

[5] Paulay, T., Park R. & Priestley M. J. N. (1978). "Reinforced concrete beam - column joint under seismic actions," **ACI Journal Proceedings.** Vol.78 (No.11): 585-593.

[6] Soleimani, D., Popov, E. P. & Bertero, V. V. (1979). "Hysteretic Behavior of Reinforced Concrete Beam - Column subassemblages," **ACI Journal Proceedings.** Vol. 76 (No.11): 1179-1195.

[7] Vintzileou, E. and Stathatos, A. (2006). "Assessment of the seismic behavior of RC columns," **Engineering Structure**. 29: 1296-1311.

[8] Sugano, S. and Nagashima T. (1985). "Structural Design and Research of Reinforced Concrete Tall Buildings," **Proceeding of the Seminar on Reinforced Concrete High-Rise Buildings in Japan with Special Concern on Aseismic Design of Beam-Column Joints (Kurose Y. and Jirsa J. O. (eds)).** Tokyo, Japan.: 85-129.

[9] Chiba, O., Fukuda, T., Toritani T., Kikuta S., Teramoto T. and Kihara, H. (1992). "Experimental and Analytical Studies on the Seismic Behavior of Reinforced Concrete Frame-wall structural Building," **Proceedings of the 10th World Conference on Earthquake Engineering.** Balkema, Rotterdam.: 3245-3251.

[10] Chaimahawan P. and Pimanmas A. (2006). "Seismic vulnerability of existing reinforced concrete buildings in Bangkok," **Proceedings of the 5th International Symposium on New Technologies for Urban Safety of Mega Cities in Asia (USMCA2006).** Thailand.: 545-555.

[11] Commite Euro-International Du Beton. (1996). **RC frames under earthquake loading.** CEB, Thomas Telford, Switzerland.

[12] American Concrete Institute. (2008). **Building code requirements for reinforced concrete-ACI318-08.** ACI, Detroit, Michigan.

[13] Sezen, H. and Moehle, J. P. (2004). “Shear strength model for lightly reinforced concrete columns,” **Journal of Structural Engineering.** ASCE, Vol.130 (No.11): 1692-1703.

[14] Applied Technology Council. (1996). **Seismic evaluation and retrofit of concrete buildings-ATC40 Volumn 1.** ATC, California.

[15] Kitayama, K., Otani, S. and Aoyama, H. (1991). **Development of design criteria for RC interior beam column joints. Design of beam-column joints for seismic resistance (James, O. J. ed.).** American Concrete Institute, SP-123: 97-123.

[16] Aoyama, H. (2001). **Design of modern highrise reinforced concrete structures.** London.: Imperial College Press.

[17] Standard Association of New Zealand. (1995). **Code of practice for design of concrete structures-NZS 3101.**

Panuwat Joyklad is a lecturer in the Department of Civil Engineering, Kasembundit University, Bangkok, Thailand. He is a secretary and member of sub-committee of Structure and Bridge of Engineering Institute of Thailand. His research activities cover a wide range of topics related to concrete structures such as advanced behavior of reinforced concrete structures, reinforced and prestressed bridge design and blast resistance of RC structure.

Amorn Pimanmas is Associate Professor in the School of Civil Engineering and Technology, SIIT, Thammasat University, Pathum Thani, Thailand.He is a chairman of sub-committee of Structure and Bridge of Engineering Institute of Thailand and also member of Council of Engineer of Thailand. He has been responsible for the design of a number of bridges and structures in Thailand and oversea-countries. He is currently involved in research for seismic retrofit and advanced behavior of concrete structures.